Detecting the chiral magnetic effect by lattice dynamics in Weyl semimetals

Zhida Song,[1] Jimin Zhao,[1] Zhong Fang,[1,2] and Xi Dai[1,2,*]

[1]*Beijing National Laboratory for Condensed Matter Physics and Institute of Physics, Chinese Academy of Sciences, Beijing 100190, China*

[2]*Collaborative Innovation Center of Quantum Matter, Beijing, 100084, China*

(Received 21 September 2016; revised manuscript received 1 December 2016; published 21 December 2016)

In the present paper, we propose that the chiral magnetic effect, the direct consequence of the presence of Weyl points in the band structure, can be detected by its coupling to certain phonon modes, which behave like pseudoscalars under point group transformations. Such coupling can generate resonance between intrinsic plasmon oscillation and the corresponding phonon modes, leading to dramatic modification of the optical response by the external magnetic field, which provides a way to study chiral magnetic effect by optical measurements.

DOI: 10.1103/PhysRevB.94.214306

I. INTRODUCTION

Weyl semimetal (WSM) [1–6] is a special type of metallic phase, which contains Weyl points (WPs), the crossing points of two nondegenerate bands, in its band structure near the Fermi level. The uniqueness of WSM lies in two different aspects, the appearance of unclosed Fermi surfaces for the surface states, Fermi arcs [5,7–13], and the abnormal response under the external fields, which can be summarized as chiral magnetic effect (CME) [14–18] and anomalous Hall effect [19–22]. Compared to anomalous Hall effect, the CME only occurs in WSM and has attracted lots of research interests in recent years.

The origin of CME can be understood from the basic electromagnetic (EM) response of a single WP. Under the external magnetic field, the low energy states around a single WP carry a finite current along the field direction due to the chirality of the zeroth Landau band [2]. It is clear that the net CME current under a static magnetic field must be zero for any equilibrium states, which can be guaranteed by the cancellation of the contributions from different WPs with opposite chiralities, and the CME can only manifest itself in the nonequilibrium states driven by the external fields [17,18,23]. For instance, the external electric field parallel to the magnetic field will pump the electrons between WPs with opposite chiralities, which is known as chiral anomaly [2,15,24], leading to particle imbalance and hence a nonzero net CME current. In the DC limit, such electron pumping will be eventually balanced by the intervalley scattering process caused by impurities. The CME/chiral anomaly leads to negative magnetoresistance along the magnetic field direction, which has been studied intensively in recent years [25–34]. In the present paper, however, we will focus on the CME in the AC limit, which will cause exotic coupling between some specific phonon mode and the CME current under the magnetic field. As will be explained in details in the following, such abnormal coupling will induce a dramatic change in the optical properties, i.e., the reflectivity, which can be detected by optical measurement directly.

II. THE PSEUDOSCALAR PHONON

According to CME, a current proportional to the magnetic field can be generated by the imbalanced chemical potentials between the WPs with opposite chiralities. The simplest way to understand CME is to consider a multi-Weyl system with different chemical potentials for each WP, where the chiral current can be expressed as

$$\mathbf{J}_{\mathrm{CME}} = \frac{e^2\mathbf{B}}{4\pi^2\hbar^2}\sum_{\mathbf{K}_i}\chi_i\mu_i \tag{1}$$

[15], where $\mathbf{K}_i$, χ_i, and μ_i denote the position, chirality, and chemical potential of the ith WP, respectively. Equation (1) can be illustrated through a simplest model containing only two WPs shown in Fig. 1. Under the external magnetic field, the low energy electronic states near the WPs become one-dimensional Landau bands, which can only disperse along the field direction as shown in Fig. 1. Since the imbalance of the chemical potentials only occurs between two different valleys, it is apparent that only the zeroth Landau band contributes to the chiral current, which can be written as:

$$\mathbf{J}_{\mathrm{CME}} = -\frac{e^2\mathbf{B}}{4\pi^2\hbar}\int_{\mathrm{occ}} dk_{\parallel}\frac{\partial\epsilon_0(k_{\parallel})}{\hbar\partial k_{\parallel}} = \frac{e^2\mathbf{B}}{4\pi^2\hbar^2}(\mu_R-\mu_L), \tag{2}$$

where $k_{\parallel}$ is the wave vector along $\mathbf{B}$, $e|\mathbf{B}|/(4\pi^2\hbar)$ is the degeneracy of each Landau level state, and $\int_{\mathrm{occ}}$ integrates over all the occupied states.

It is well known that the imbalanced chemical potentials can be induced by chiral anomaly effect [2,15,24], which pumps electrons between WPs with opposite chiralities. Besides chiral anomaly, strain has also been proposed as a method to introduce such imbalance [35]. In the present paper, we propose that such imbalance and hence the chiral current can also be induced by the deformation potentials associated with some optical phonon modes. Since the generic WSM contains multiple pairs of WPs, it is important to know that for a given phonon mode the contributions from different pairs of WPs will cancel each other or not, which is fully determined by the crystal symmetry. In the main text we will mostly focus on the conclusions of such group theory analysis and leave the mathematical proof in the Appendix. For the sake of simplicity, in the current study we only consider the nondegenerate optical phonon modes in the long wavelength

*daix@aphy.iphy.ac.cn

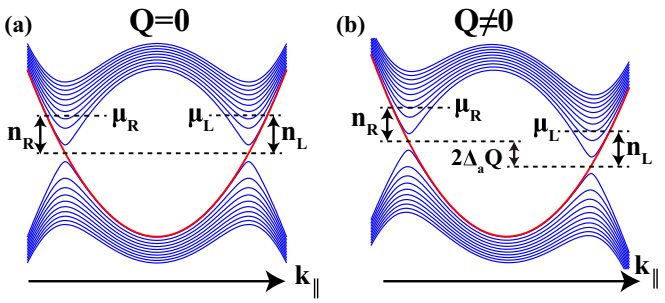

FIG. 1. Landau bands and deformation potential in a two WPs model. The red and blue lines represent the zeroth (chiral) Landau band and other Landau bands, respectively. Chiral charge density is defined as $n_a = n_R - n_L$. (a) is the case of $Q = 0$ and (b) is the case of $Q \neq 0$.

limit, which form one-dimensional representations of the little group at the Γ point. To the leading order, the electron-phonon coupling for a specific phonon mode can be expressed as:

$$\hat{H}_{ep} = \frac{1}{V}\sum_{\mathbf{K}_i\mathbf{p}} \hat{\psi}^{\dagger}_{\mathbf{K}_i+\mathbf{p}} \Delta_{\mathbf{K}_i,Q} \hat{\psi}_{\mathbf{K}_i+\mathbf{p}} Q, \tag{3}$$

which describes the energy shifts of the WPs by the deformation potential owing to the phonon mode Q. The summation over $\mathbf{p}$ only includes the low energy states around each WP. In the present paper, we consider the AC limit together with the clean limit, where the relaxation rate due to the impurity scattering is much less than the typical phonon or plasmon frequency. Therefore, for simplicity we neglect the impurity scattering and only consider the dynamical effect. Consider that the system deforms from $Q = 0$ [Fig. 1(a)] to $Q \neq 0$ [Fig. 1(b)]. Since the carrier relaxation is neglected here, the occupation of the Landau bands does not follow the change of the Hamiltonian, leading to the imbalanced chemical potential $\mu_i = \Delta_{\mathbf{K}_i,Q} Q$. Then according to Eq. (1), the CME current induced by the deformation potential caused by the phonon mode Q can be obtained as:

$$\mathbf{J}_{\mathrm{CME},Q} = \frac{N_W e^2 \mathbf{B}}{4\pi^2\hbar^2} \Delta_{a,Q} Q, \tag{4}$$

where $\Delta_{a,Q} = \frac{1}{N_W}\sum_i^{N_W} \chi_i \Delta_{\mathbf{K}_i,Q}$ and N_W is the number of WPs.

A phone mode Q can couple to the CME current only if $\Delta_{a,Q}$ does not vanish, which sets the constraint for the allowed phonon modes. From the symmetry point of view, all the WSM materials can be divided into two classes by whether or not their space groups contain improper rotations, such as the inversion or mirror operators. As proved rigorously in Appendix A, if the space group does not contain any improper rotations, the symmetry allowed phonon modes are those A_1 modes, which behave as scalars under the little group at the Γ point. Up to now most of the WSM materials do have improper rotations in the space groups and thus belong to the latter class. In this class, the phonon modes that couple to CME must behave as pseudoscalars under the point group transformations. In other words, these phonon modes must keep identity under all the proper rotations and change signs under all the improper rotations. Such phonon modes are called pseudoscalar phonons in this paper, which can be either polarized or unpolarized. Apparently, if a pseudoscalar mode is polarized its polarization vector must be parallel (perpendicular) to any symmetry axes (mirrors) of the point group. As a result, as long as there are two or more nonparallel rotation axes or mirror normals the allowed phonon mode cannot be polarized. The above conclusions can be easily derived from the invariance of the Hamiltonian (3) under all the point group transformations, which is described in detail in Appendix A. In Appendix B we also apply this criterion to some Dirac semimetals and WSMs studied recently in the literature and find that in $HgCr_2Se_4$ [36], Cd_3As_2 [37], and AMo_3X_3 [38] the symmetry allowed phonon modes do exist. In the following, we will illustrate how the coupling between the pseudoscalar phonon and the CME affects the lattice dynamics and hence manifests itself in the optical response.

III. EQUATIONS OF MOTION (EOMs)

From Eq. (4), we can find that in WSM a current along the external magnetic field $\mathbf{B}$ can be induced by the motion of the pseudoscalar phonon mode. Such a CME current will generate charge accumulation at the sample boundaries and cause an internal electric field $\mathbf{E}$, which leads to intervalley electron pumping under the magnetic field $\mathbf{B}$ due to the chiral anomaly. Therefore in such a system, the EOMs for pseudoscalar phonon mode Q, chiral charge density defined as $n_a = \sum_i^{N_W} \chi_i n_i$ [Fig. 1(b)], as well as the electric field $\mathbf{E}$ are all coupled together, leading to quite unusual EM responses. In the present paper, we will mainly focus on the EOMs for the unpolarized phonon mode and briefly discuss the possible effects related to the polarized phonon modes thereafter. Tracing out the electronic degrees of freedom in Eq. (3), we obtain the effective Lagrangian density for the phonon as:

$$\mathcal{L} = \frac{M_{ph}}{2\Omega}\dot{Q}^2 - \frac{M_{ph}\omega_{ph}^2}{2\Omega}Q^2 - \Delta_a n_a Q, \tag{5}$$

where M_{ph} is the effective mass of the ions, ω_{ph} is the phonon frequency, and Ω is the unit cell volume. Then the EOM of Q can be obtained as:

$$\ddot{Q} + \omega_{ph}^2 Q + \frac{\Delta_a \Omega}{M_{ph}} n_a = 0. \tag{6}$$

On the other hand, according to Refs. [15,24]the low energy electronic dynamics near the WPs leads to the chiral anomaly, the electron pumping between WPs with opposite chiralities, which can be expressed as:

$$\dot{n}_a = \frac{e^2 N_W}{4\pi^2\hbar^2}\mathbf{E}\cdot\mathbf{B}. \tag{7}$$

Next we consider the EOM for the EM wave propagating in the WSM, which can be written as

$$\ddot{\mathbf{D}} + \dot{\mathbf{J}} + \frac{1}{\mu}\nabla(\nabla\cdot\mathbf{E}) - \frac{1}{\mu}\nabla^2\mathbf{E} = 0. \tag{8}$$

In WSM $\mathbf{D}$ can be simply set as $\epsilon_0\kappa\mathbf{E}$ where κ is dielectric constant in the high frequency limit, while the current $\mathbf{J}$

contains multiple terms with different origins, which can be written as $\mathbf{J}_{\text{total}} = \mathbf{J}_{\text{op}} + \mathbf{J}_{\text{H}} + \mathbf{J}_{\text{CME}} + \mathbf{J}_{\text{AH}}$. The first two terms are the optical current $\mathbf{J}_{\text{op},i} = \sigma_i(\omega,\mathbf{q})\mathbf{E}_i$ (where i distinguishes the transversal and longitudinal responses) and the Hall current $\mathbf{J}_{\text{H}} = \sigma_{\text{H}}(\omega,\mathbf{q})\mathbf{E}\times\mathbf{B}$, which exist in all metallic systems. In addition, there are two novel components in a WSM, the CME and anomalous Hall currents. In the clean limit, further considering the nonzero chiral charge n_a, the imbalanced chemical potential for the zeroth Landau level can be expressed as $\Delta\mu_0 = N_W\Delta_a Q + n_a/\nu_D$, where $\nu_D = \frac{e|\mathbf{B}|}{4\pi^2\hbar^2 v_F}$ is the density of states of a single zeroth Landau band. The two terms contained in $\Delta\mu_0$ describe the pseudoscalar phonon contribution and chiral anomaly contribution, respectively. Thus the total CME current is explicitly written as:

$$\mathbf{J}_{\text{CME}} = \frac{e^2\mathbf{B}}{4\pi^2\hbar^2}\left(N_W\Delta_a Q + \frac{n_a}{\nu_D}\right). \tag{9}$$

The anomalous Hall current can be expressed as $\mathbf{J}_{\text{AH}} = \frac{e^2}{\hbar}\mathbf{E}\times\mathbf{d}$, where $\mathbf{d} = \int\frac{d^3\mathbf{k}}{(2\pi)^3}n_F(\epsilon_{\mathbf{k}})\boldsymbol{\Omega}_{\mathbf{k}}$ is the integral of the Berry curvature contributed by all the occupied bands over the Brillouin zone. Including all the four different origins of the current in Eq. (8), we obtain the coupled equations (6), (7), and (8) for the pseudoscalar phonon mode Q, chiral charge density n_a, and the electric field $\mathbf{E}$, which can be solved under different conditions leading to several novel optical properties introduced below.

IV. PHYSICAL CONSEQUENCES

The above EOMs give a mechanism to couple the EM wave with the pseudoscalar phonons through CME, which only exists under the external magnetic field. If the particular pseudoscalar phonon mode is polarized, the additional coupling caused by CME only modifies the coupling strength between the two, while if the pseudoscalar phonon mode is unpolarized, it can now couple to the EM wave through the CME, which will generate a dramatic change in the optical response near the phonon frequency. In other words, the originally optical inactive phonon mode can become active under the external magnetic field due to the CME. In this present paper, we will mainly focus on the unpolarized phonon modes and only briefly discuss the polarized phonon modes thereafter, because the effect in the former case is more dramatic. To avoid additional contributions from both ordinary and anomalous Hall effects, we always set the external magnetic field $\mathbf{B}$ to be parallel to the vector $\mathbf{d}$ (if there is a nonzero $\mathbf{d}$) and consider the polarization of the EM mode to be along the magnetic field. In total there are two EM modes, which are free from Hall effects and will be studied in detail below.

The first one is the transverse mode describing an EM wave with wave vector $\mathbf{q}$ being perpendicular and polarization direction being parallel to the magnetic field $\mathbf{B}$, as shown in Fig. 2(a). The EOM for the electric field in such a situation can be simplified as

$$-\kappa\omega^2 E_{T1} - i\frac{\omega}{\epsilon_0}\sigma_T(\omega\mathbf{q})E_{T1} + \frac{1}{\mu\epsilon_0}\mathbf{q}^2 E_{T1} - i\frac{\omega e^2 B}{4\pi^2\epsilon_0\hbar^2}\left(N_W\Delta_a Q + \frac{n_a}{\nu_D}\right) = 0, \tag{10}$$

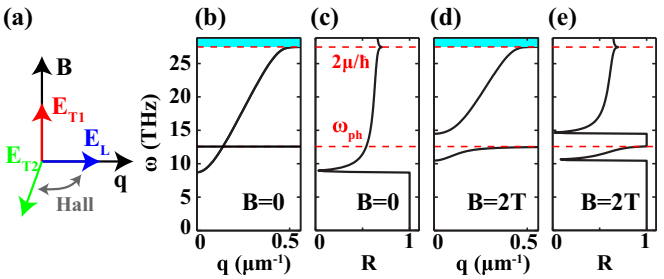

FIG. 2. EM wave coupled with unpolarized pseudoscalar phonon. (a) illustrates the fields configuration, which ensures that the mode coupled with CME current (E_{T1}) and is free from Hall effects. (b) and (c) are the numerically calculated dispersion and reflectivity for E_{T1} at $\mathbf{B} = 0$. (d) and (e) are the dispersion and reflectivity at $\mathbf{B} = 2$ T. The cyan areas are the interband single particle excitation zones [39].

where σ_T denotes the transverse optical conductivity [39]. The effective dielectric function in this case can be obtained by substituting the solution of Eqs. (6) and (7) into Eq. (10), which can be written as

$$\epsilon_{r,T} = \kappa + i\frac{\sigma_T(\omega\mathbf{q})}{\omega\epsilon_0} - \frac{e^4B^2}{16\pi^4\hbar^4\epsilon_0\omega^2}\left[\frac{N_W}{\nu_D} + \frac{N_W^2\Delta_a^2\Omega}{M_{ph}(\omega^2-\omega_{ph}^2)}\right] = \epsilon_{r,T}^0 - \frac{e^4B^2}{16\pi^4\hbar^4\epsilon_0\omega^2}\left[\frac{N_W}{\nu_D} + \frac{N_W^2\Delta_a^2\Omega}{M_{ph}(\omega^2-\omega_{ph}^2)}\right], \tag{11}$$

where $\epsilon_{r,T}^0$ is the original dielectric function without magnetic field. The above solution indicates that through CME the photon with the polarization along the field direction can hybridize with the unpolarized pseudoscalar phonon to form a special type of polariton mode, which can only exist under the magnetic field. If the phonon frequency ω_{ph} is higher than the plasmon frequency ω_{pl}, as shown in Fig. 2(b), without the magnetic field there is a level crossing between E_{T1} and Q at frequency ω_{ph} and momentum $\hbar\mathbf{q}_0$, which becomes anticrossing under the magnetic field through the CME. By solving the equation $\epsilon_{r,T} = c^2\mathbf{q}^2/\omega^2$ to the first order of $\mathbf{B}$ and Δ_a, we can get the hybridization gap between the photonlike and phononlike branches to be

$$\Delta\omega \approx \frac{e^2N_W\Delta_a|\mathbf{B}|}{\pi^2\hbar^2}\times\sqrt{\frac{\Omega}{8\epsilon_0 M_{ph}\omega_{ph}^3\left(\frac{2\epsilon_{r,T}^0}{\omega_{ph}} + \frac{\partial\epsilon_{r,T}^0}{\partial\omega}\right)_{\omega_{ph},\mathbf{q}_0}}}. \tag{12}$$

The existence of such a CME induced polariton mode can be inferred from the dramatic modification of the reflectivity under the magnetic field, which can be written as $R = |\frac{\sqrt{\epsilon_r}-1}{\sqrt{\epsilon_r}+1}|^2$ [41]. For example, as ω approaches ω_{ph} the last term in Eq. (11) will diverge, leading to an additional peak in the reflectivity.

We further apply numerical calculations for the CME induced polariton modes using the typical parameters for the semiconductor or semimetal materials, which are $N_W = 4$, $v_F = 2.2\times10^5$ m/s, $\kappa = 15$, $\Delta_a = 8$ eV/Å, $M_{ph} = 90$ u, $\omega_{ph} = 12.6$ THz, and $\Omega = 2021$ Å^3. The Fermi momentum has been chosen as $p_F = 0.0063$ Å^{-1}. The dispersion of the

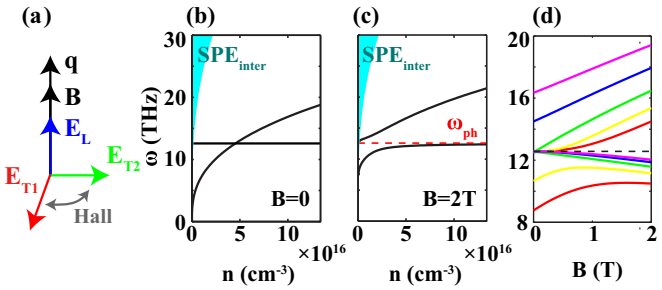

FIG. 3. Plasmon coupled with unpolarized pseudoscalar phonon. (a) illustrates the fields configuration, which ensures that the mode coupled with CME current (E_L) is free from Hall effect. (b) and (c) are the eigenfrequencies of the coupled modes as functions of carrier density at $\mathbf{B} = 0$ and $\mathbf{B} = 2$ T, respectively, where the cyan areas are the interband single particle excitation zones [40]. In (d) we plot the eigenfrequencies of the coupled modes as functions of the magnetic field. Different colored lines represent different intrinsic plasmon frequencies (carriers densities).

polariton modes and the reflectivity of light are calculated and shown in Fig. 2. A CME induced hybridization gap between the phonon and photonlike branches can be found clearly under the magnetic field, as shown in Fig. 2(d), which generates an additional peak in the optical reflectivity after the plasmon edge, as illustrated in Fig. 2(e).

The second EM mode, that is free from the Hall effects, is the longitudinal or plasmonic mode [42–44] with wave vector and polarization direction both being parallel to the magnetic field. The EOM can then be simplified to

$$-\kappa\omega^2 E_L - i\frac{\omega}{\epsilon_0}\sigma_L(\omega\mathbf{q})E_L - i\frac{\omega e^2 B}{4\pi^2\epsilon_0\hbar^2}\left(N_W\Delta_a Q + \frac{n_a}{\nu_D}\right) = 0, \tag{13}$$

where σ_L denotes the longitudinal conductivity. The effective dielectric function for E_L is similar with Eq. (11) except that σ_T is replaced by σ_L. Similar to the polariton case, the CME will generate coupling between the unpolarized pseudoscalar phonon and the plasmon modes, which are otherwise completely decoupled without the CME. Similarly we can obtain the hybridization gap between the two branches as

$$\Delta\omega \approx \frac{e^2 N_W \Delta_a |\mathbf{B}|}{\pi^2\hbar^2}\sqrt{\frac{\Omega}{8\epsilon_0 M_{ph}\omega_{ph}^3\kappa\left.\frac{\partial\epsilon_{r,L}^0}{\partial\omega}\right|_{\omega_{ph},\mathbf{q}_0}}}, \tag{14}$$

where $\epsilon_{r,L}^0$ is the original longitudinal dielectric function without magnetic field [40]. The similar numerical calculations for the coupled plasmon and phonon modes have been carried out using the same parameters introduced above, and the results are shown in Fig. 3, where the hybridization between the plasmon and phonon modes can be induced only with the finite magnetic field. Such mixed modes under magnetic field can be detected by the Raman scattering with the proper setup.

In the end, we briefly discuss the situation for the polarized pseudoscalar phonon modes. We list the four different configurations in Fig. 4 as examples and always set as $\mathbf{B}\|\mathbf{d}$ if there is a nonzero $\mathbf{d}$. In Fig. 4(a), the phonon mode couples to the EM

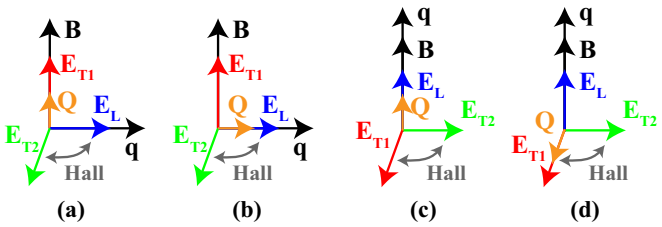

FIG. 4. EM modes coupled with polarized pseudoscalar phonon.

mode E_{T1} because their polarization directions are parallel to each other. The CME enhances such coupling and modifies the dispersion of the polariton modes in this case. The situation in Fig. 4(b) is more complicated. The two transverse EM modes, the longitudinal plasmon mode, and the pseudoscalar phonon mode are all coupled together under the magnetic field due to the combination of the Hall effect and CME. The case in Fig. 4(c) is similar with the case in Fig. 4(a), in which the CME enhances the coupling strength between Q and E_L. The case in Fig. 4(d) is as complicated as the case in Fig. 4(b) because all the modes are coupled together.

V. CONCLUSIONS

In summary, a special type of phonon mode, which behaves as pseudoscalar under improper rotation, is proposed to be coupled to the EM dynamics in the WSMs or Dirac semimetals. If such a pseudoscalar phonon mode is unpolarized, it will become optically active under the external magnetic field, manifesting the CME in these materials. Such CME induced phonon-EM wave coupling can be detected easily by the optical reflectivity spectroscopy near the phonon frequency, providing an experimental way to study the CME in topological semimetals.

Note added. Recently, we were informed that partial results in our paper were also obtained independently in another work Ref. [54].

ACKNOWLEDGMENTS

We acknowledge the support from National Natural Science Foundation of China, the National 973 program of China (Grant No. 2013CB921700), and the "Strategic Priority Research Program (B)" of the Chinese Academy of Sciences (Grant No. XDB07020100).

APPENDIX A: PSEUDOSCALAR PHONON AND CME CURRENT

In this section we will prove that only a pseudoscalar phonon can be coupled with the CME current. The CME current caused by imbalanced chemical potential between Weyl nodes is described as Eq. (1), and the interaction between electrons, a phonon mode Q, is described in Eq. (3). On one hand, Q must form a one-dimensional representation of the little group at Γ (denoted as G):

$$\forall g \in G, \quad gQg^{-1} = D_Q(g)Q. \tag{A1}$$

On the other hand, the invariance of $\hat{H}_{ep}$ under group G implies:

$$\begin{aligned}&\frac{1}{V}\sum_{\mathbf{K}_i\mathbf{p}}\hat{\psi}^{\dagger}_{\mathbf{K}_i+\mathbf{p}}\Delta_{\mathbf{K}_i}\hat{\psi}_{\mathbf{K}_i+\mathbf{p}}Q\\&=\frac{1}{V}\sum_{\mathbf{K}_i\mathbf{p}}g\hat{\psi}^{\dagger}_{\mathbf{K}_i+\mathbf{p}}\Delta_{\mathbf{K}_i}\hat{\psi}_{\mathbf{K}_i+\mathbf{p}}Qg^{-1}\\&=\frac{1}{V}\sum_{\mathbf{K}_i\mathbf{p}}\hat{\psi}^{\dagger}_{\mathbf{K}_i+\mathbf{p}}\Delta_{g^{-1}\mathbf{K}_i}\hat{\psi}_{\mathbf{K}_i+\mathbf{p}}gQg^{-1}.\end{aligned}\tag{A2}$$

Combining Eq. (A1) and Eq. (A2) we have:

$$\Delta_{g\mathbf{K}_i}=D_Q(g)\Delta_{\mathbf{K}_i}.\tag{A3}$$

Assume there is a right-hand Weyl node at $\mathbf{K}$, by symmetry principle we know there will be a right-(left)hand Weyl node at $g\mathbf{K}$ if $\det g=1$ ($\det g=-1$). Thus the net imbalanced chemical potential contributed by Q is:

$$\begin{aligned}\Delta\mu_Q&=\sum_{\mathbf{K}_i}{}'\frac{1}{|H^{\mathbf{K}_i}|}\sum_{g\in G}\det g\cdot\Delta_{g\mathbf{K}_i}\cdot Q\\&=\sum_{\mathbf{K}_i}{}'\Delta_{\mathbf{K}_i}\frac{1}{|H^{\mathbf{K}_i}|}\sum_{g\in G}\det g\cdot D_Q(g)\cdot Q,\end{aligned}\tag{A4}$$

where the summation $\sum'$ goes through all nonequivalent Weyl nodes and $H^{\mathbf{K}_i}$ is the little group of $\mathbf{K}_i$. The denominator $|H^{\mathbf{K}_i}|$ in Eq. (A4) is used to cancel the multiplicity from $\mathbf{K}_i$-invariant operations. Since $\det g$ itself is an irreducible representation of G, orthogonality theorem ensures that only a pseudoscalar phonon, i.e., $D_Q(g)=\det g$, can induce net $\Delta\mu_Q$. Therefore the CME current, according to Eq. (1), is also only coupled with a pseudoscalar phonon. We emphasize that the general proof above also applies to other fields linearly coupled to Weyl fermions.

APPENDIX B: PSEUDOSCALAR PHONONS IN MATERIALS

In this section we will discuss the pseudoscalar phonons in materials. Firstly we give a criterion for the existence of pseudoscalar phonons. As phonon modes are completely determined by crystal structure, we can give a criterion based only on symmetry principles. Assume there are L nonequivalent occupied Wyckoff sites, each of which has a site symmetry group (SSG) H^a ($a=1\cdots L$). G can be decomposed as cosets of H^a:

$$G=s_1H^a+s_2H^a+\cdots\tag{B1}$$

It should be noticed that the point group operations may contain fractional translations in nonsymmorphic systems. For the ath kind of Wyckoff sites, H^a keeps each site invariant and s_i interchanges them, so there are $\frac{|G|}{|H^a|}$ atoms in this kind. Thus the mechanical representation formed by the displacements configuration is:

$$D(g)=\bigoplus_{a=1}^{L}\left[D^a_{\text{int}}(s)\otimes D^a_{\text{O(3)}}(h)\right]\tag{B2}$$

where:

$$s\cdot h=g\quad s\in G/H^a\quad h\in H^a\tag{B3}$$

TABLE I. Pseudoscalar phonons in Weyl and Dirac semimetals.

		Materials	Space Group	Little Group Group at Γ	Relevant Wyckoff Site	SSG	Pseudo-scalar Phonon[a]	Polarized
Weyl	non-magnetic	$A\text{Bi}_{1-x}\text{Se}_x\text{Te}_3$ [45]	160	C_{3v}	–	–	–	–
		BiTeI under pressure [45]	156	C_{3v}	–	–	–	–
		Se/Te under pressure [46]	152/153	D_3	$3a$	C_2	A_1	No
		TaAs [7,8]	109	C_{4v}	–	–	–	–
	magnetic	$A_2\text{Ir}_2\text{O}_7$ [5]	227.131[b]	$\mathcal{O}_h$[c]	–	–	–	–
		HgCr_2Se_4 [36]	141.557[b]	$\mathcal{D}_{4h}$[c]	$8c$, $16h$	C_{2h}, C_s	$2\times A_{1u}$	No
Dirac	Class I[d]	Cu_3PdN [47]	221	O_h	–	–	–	–
		$A_3\text{Bi}$ [48]	194	D_{6h}	–	–	–	–
		BaAuBi-family [38]	194	D_{6h}	–	–	–	–
		LiGaGe-family [38]	186	C_{6v}	–	–	–	–
		SrSn_2As_2[38]	160	C_{3v}	–	–	–	–
		Cd_3As_2 [37]	137	D_{4h}	$3\times 8g$, $8f$	C_s, C_2	$4\times A_{1u}$	No
		Cd_3As_2 [37]	110	C_{4v}	$9\times 16b$, $2\times 8a$	C_1, C_2	$29\times A_2$	No
	Class II	β-cristobalite BiO_2 [49]	227	O_h	–	–	–	–
		HfI_3 [38]	193	D_{6h}	–	–	–	–
		$A\text{Mo}_3X_3$-family [38]	176	C_{6h}	$2\times 6h$	C_s	$2\times A_u$	Yes
		Distorted Spinel [50]	74	D_{2h}	$4a$, $4d$, $8h$, $8i$	C_{2h}, C_{2h}, C_s, C_s	$4\times A_u$	No

[a]The symbol for irreducible representations follow Ref. [51]. The prefactor is the number of pseudoscalar phonon modes. "-" means there is no pseudoscalar phonon.

[b]The magnetic space group is referred to Ref. [52].

[c]The magnetic little group is defined as $\mathcal{O}_h=T_h+\mathcal{T}\cdot(O_h-T_h)$ and $\mathcal{D}_{4h}=C_{4h}+\mathcal{T}\cdot(D_{4h}-C_{4h})$ respectively, where $\mathcal{T}$ is the time reversal operator.

[d]The classification follows Ref. [53].

and $D^a_{\rm int}(s)$ is the $\frac{|G|}{|H^a|}\times\frac{|G|}{|H^a|}$ interchange matrix, $D^a_{\rm O(3)}(h)$ is just the O(3) rotation matrix of h. Then we can apply the orthogonality theorem to calculate the multiplicity of pseudoscalar representation. By recognizing that $D^a_{\rm int}(s)$ is off diagonal unless s equals to identity, the multiplicity λ can be simplified to:

$$\lambda = \sum_{a=1}^{L}\frac{1}{|G|}\sum_{s\in G/H^a}\sum_{h\in H^a}\det(s\cdot h)\mathrm{tr}\left[D^a_{\rm int}(s)\otimes D^a_{\rm O(3)}(h)\right]$$
$$= \sum_{a=1}^{L}\frac{1}{|H^a|}\sum_{h\in H^a}\det(h)\cdot\mathrm{tr}\left[D^a_{\rm O(3)}(h)\right], \quad \text{(B4)}$$

which indicates that λ is determined only by the SSG of occupied Wyckoff sites. The SSGs that can contribute to Eq. (B4) are easy to exhaust, and we classify them into two classes:

$$\mathcal{H}_3 = \{C_1, C_i\} \quad \text{(B5)}$$

$$\mathcal{H}_1 = \{C_2, C_3, C_4, C_6, C_{2h}, C_{3h}, C_{4h}, C_{6h}, C_s, S_4, S_6\}. \quad \text{(B6)}$$

The symbol for point group follows Ref. [51]. Each group in $\mathcal{H}_3$ will contribute 3 in Eq. (B4), and each group in $\mathcal{H}_1$ will contribute 1 in Eq. (B4). This can be understood in a quite intuitive perspective: As a pseudoscalar mode the displacement of each atom must be parallel (perpendicular) to any symmetry axes (mirrors) in the site group, so as long as there are two or more nonparallel axes or mirror normals the displacement must be zero. (The symmetry axis here represents both the rotation and rotation-reflection axis). Indeed $\mathcal{H}_3$ are those groups which have no symmetry axes or mirrors, and $\mathcal{H}_1$ are those groups which have only one direction of symmetry axes or mirror normals. Therefore we achieve the criterion: The existence of pseudoscalar phonon is equivalent with the existence of occupied Wyckoff sites with SSGs in $\mathcal{H}_3\cup\mathcal{H}_1$. The number of pseudoscalar modes can be simply counted as the number of nonequivalent $\mathcal{H}_1$ Wyckoff sites plus three times the number of nonequivalent $\mathcal{H}_3$ Wyckoff sites. We list the pseudoscalar phonons in some predicted Weyl or Dirac semimetals in Table I.

[1] H. Weyl, Z. Phys. **56**, 330 (1929).
[2] H. B. Nielsen and M. Ninomiya, Phys. Lett. B **130**, 389 (1983).
[3] G. E. Volovik, *The Universe in a Helium Droplet* (Clarendon Press, Oxford University Press, New York, 2003).
[4] S. Murakami, New J. Phys. **9**, 356 (2007).
[5] X. Wan, A. M. Turner, A. Vishwanath, and S. Y. Savrasov, Phys. Rev. B **83**, 205101 (2011).
[6] A. A. Burkov and L. Balents, Phys. Rev. Lett. **107**, 127205 (2011).
[7] H. Weng, C. Fang, Z. Fang, B. A. Bernevig, and X. Dai, Phys. Rev. X **5**, 011029 (2015).
[8] S.-M. Huang, S.-Y. Xu, I. Belopolski, C.-C. Lee, G. Chang, B. Wang, N. Alidoust, G. Bian, M. Neupane, C. Zhang, S. Jia, A. Bansil, H. Lin, and M. Z. Hasan, Nat. Commun. **6**, 7373 (2015).
[9] A. C. Potter, I. Kimchi, and A. Vishwanath, Nat. Commun. **5**, 5161 (2014).
[10] B. Q. Lv, N. Xu, H. M. Weng, J. Z. Ma, P. Richard, X. C. Huang, L. X. Zhao, G. F. Chen, C. E. Matt, F. Bisti, V. N. Strocov, J. Mesot, Z. Fang, X. Dai, T. Qian, M. Shi, and H. Ding, Nat. Phys. **11**, 724 (2015).
[11] B. Q. Lv, S. Muff, T. Qian, Z. D. Song, S. M. Nie, N. Xu, P. Richard, C. E. Matt, N. C. Plumb, L. X. Zhao, G. F. Chen, Z. Fang, X. Dai, J. H. Dil, J. Mesot, M. Shi, H. M. Weng, and H. Ding, Phys. Rev. Lett. **115**, 217601 (2015).
[12] S.-Y. Xu, N. Alidoust, I. Belopolski, Z. Yuan, G. Bian, T.-R. Chang, H. Zheng, V. N. Strocov, D. S. Sanchez, G. Chang, C. Zhang, D. Mou, Y. Wu, L. Huang, C.-C. Lee, S.-M. Huang, B. Wang, A. Bansil, H.-T. Jeng, T. Neupert, A. Kaminski, H. Lin, S. Jia, and M. Zahid Hasan, Nat. Phys. **11**, 748 (2015).
[13] S.-Y. Xu, I. Belopolski, N. Alidoust, M. Neupane, G. Bian, C. Zhang, R. Sankar, G. Chang, Z. Yuan, C.-C. Lee, S.-M. Huang, H. Zheng, J. Ma, D. S. Sanchez, B. Wang, A. Bansil, F. Chou, P. P. Shibayev, H. Lin, S. Jia, and M. Z. Hasan, Science **349**, 613 (2015).
[14] K. Fukushima, D. E. Kharzeev, and H. J. Warringa, Phys. Rev. D **78**, 074033 (2008).
[15] D. T. Son and N. Yamamoto, Phys. Rev. Lett. **109**, 181602 (2012).
[16] A. A. Zyuzin and A. A. Burkov, Phys. Rev. B **86**, 115133 (2012).
[17] Y. Chen, S. Wu, and A. A. Burkov, Phys. Rev. B **88**, 125105 (2013).
[18] M. M. Vazifeh and M. Franz, Phys. Rev. Lett. **111**, 027201 (2013).
[19] Z. Fang, N. Nagaosa, K. S. Takahashi, A. Asamitsu, R. Mathieu, T. Ogasawara, H. Yamada, M. Kawasaki, Y. Tokura, and K. Terakura, Science **302**, 92 (2003).
[20] D. Xiao, M.-C. Chang, and Q. Niu, Rev. Mod. Phys. **82**, 1959 (2010).
[21] K.-Y. Yang, Y.-M. Lu, and Y. Ran, Phys. Rev. B **84**, 075129 (2011).
[22] I. Sodemann and L. Fu, Phys. Rev. Lett. **115**, 216806 (2015).
[23] S. Zhong, J. Orenstein, and J. E. Moore, Phys. Rev. Lett. **115**, 117403 (2015).
[24] M. A. Stephanov and Y. Yin, Phys. Rev. Lett. **109**, 162001 (2012).
[25] D. T. Son and B. Z. Spivak, Phys. Rev. B **88**, 104412 (2013).
[26] K.-S. Kim, H.-J. Kim, and M. Sasaki, Phys. Rev. B **89**, 195137 (2014).
[27] A. A. Burkov, Phys. Rev. Lett. **113**, 247203 (2014).
[28] A. A. Burkov, Phys. Rev. B **91**, 245157 (2015).
[29] H.-J. Kim, K.-S. Kim, J.-F. Wang, M. Sasaki, N. Satoh, A. Ohnishi, M. Kitaura, M. Yang, and L. Li, Phys. Rev. Lett. **111**, 246603 (2013).
[30] X. Huang, L. Zhao, Y. Long, P. Wang, D. Chen, Z. Yang, H. Liang, M. Xue, H. Weng, Z. Fang, X. Dai, and G. Chen, Phys. Rev. X **5**, 031023 (2015).
[31] J. Xiong, S. K. Kushwaha, T. Liang, J. W. Krizan, M. Hirschberger, W. Wang, R. J. Cava, and N. P. Ong, Science **350**, 413 (2015).

[32] C.-L. Zhang, S.-Y. Xu, I. Belopolski, Z. Yuan, Z. Lin, B. Tong, G. Bian, N. Alidoust, C.-C. Lee, S.-M. Huang, T.-R. Chang, G. Chang, C.-H. Hsu, H.-T. Jeng, M. Neupane, D. S. Sanchez, H. Zheng, J. Wang, H. Lin, C. Zhang, H.-Z. Lu, S.-Q. Shen, T. Neupert, M. Z. Hasan, and S. Jia, Nat. Commun. **7**, 10735 (2016).

[33] C.-Z. Li, L.-X. Wang, H. Liu, J. Wang, Z.-M. Liao, and D.-P. Yu, Nat. Commun. **6**, 10137 (2015).

[34] H. Li, H. He, H.-Z. Lu, H. Zhang, H. Liu, R. Ma, Z. Fan, S.-Q. Shen, and J. Wang, Nat. Commun. **7**, 10301 (2016).

[35] A. Cortijo, D. Kharzeev, K. Landsteiner, and M. A. H. Vozmediano, arXiv:1607.03491.

[36] G. Xu, H. Weng, Z. Wang, X. Dai, and Z. Fang, Phys. Rev. Lett. **107**, 186806 (2011).

[37] Z. Wang, H. Weng, Q. Wu, X. Dai, and Z. Fang, Phys. Rev. B **88**, 125427 (2013).

[38] Q. D. Gibson, L. M. Schoop, L. Muechler, L. S. Xie, M. Hirschberger, N. P. Ong, R. Car, and R. J. Cava, Phys. Rev. B **91**, 205128 (2015).

[39] P. E. C. Ashby and J. P. Carbotte, Phys. Rev. B **89**, 245121 (2014).

[40] M. Lv and S.-C. Zhang, Int. J. Mod. Phys. B **27**, 1350177 (2013).

[41] N. W. Ashcroft and N. D. Mermin, *Solid State Physics* (Holt, Rinehart and Winston, New York, 1976).

[42] I. Panfilov, A. A. Burkov, and D. A. Pesin, Phys. Rev. B **89**, 245103 (2014).

[43] J. Zhou, H.-R. Chang, and D. Xiao, Phys. Rev. B **91**, 035114 (2015).

[44] B. Z. Spivak and A. V. Andreev, Phys. Rev. B **93**, 085107 (2016).

[45] J. Liu and D. Vanderbilt, Phys. Rev. B **90**, 155316 (2014).

[46] M. Hirayama, R. Okugawa, S. Ishibashi, S. Murakami, and T. Miyake, Phys. Rev. Lett. **114**, 206401 (2015).

[47] R. Yu, H. Weng, Z. Fang, X. Dai, and X. Hu, Phys. Rev. Lett. **115**, 036807 (2015).

[48] Z. Wang, Y. Sun, X.-Q. Chen, C. Franchini, G. Xu, H. Weng, X. Dai, and Z. Fang, Phys. Rev. B **85**, 195320 (2012).

[49] S. M. Young, S. Zaheer, J. C. Y. Teo, C. L. Kane, E. J. Mele, and A. M. Rappe, Phys. Rev. Lett. **108**, 140405 (2012).

[50] J. A. Steinberg, S. M. Young, S. Zaheer, C. L. Kane, E. J. Mele, and A. M. Rappe, Phys. Rev. Lett. **112**, 036403 (2014).

[51] S. L. Altmann and P. Herzig, *Point-Group Theory Tables* (Clarendon Press, Gloucestershire, 1994).

[52] S. V. Gallego, E. S. Tasci, G. d. l. Flor, J. M. Perez-Mato, and M. I. Aroyo, J. Appl. Crystallogr. **45**, 1236 (2012).

[53] B.-J. Yang and N. Nagaosa, Nat. Commun. **5**, 4898 (2014).

[54] P. Rinkel, P. L. S. Lopes, and I. Garate, arXiv:1610.03073.